

# An analytically iterative method for solving problems of cosmic ray modulation

Yuriy L. Kolesnyk,<sup>1</sup> Pavol Bobik,<sup>2</sup> Boris A. Shakhov,<sup>1</sup> Marian Putis<sup>2</sup>

<sup>1</sup>*Main Astronomical Observatory, National Academy of Sciences of Ukraine, 27, Akademika Zabolotnoho St., 03680, Kyiv, Ukraine*

<sup>2</sup>*Institute of Experimental Physics, Watsonova 47, 04001 Kosice, Slovakia*

Accepted 2017 May 11. Received 2017 May 11; in original form 2017 February 13

## ABSTRACT

The development of an analytically iterative method for solving steady-state as well as unsteady problems of Cosmic Ray (CR) modulation is proposed. Iterations for obtaining the solutions are constructed for the spherically symmetric form of the CR propagation equation. The main solution of the considered problem consists of the zero order solution that is obtained during the initial iteration and amendments that may be obtained by subsequent iterations. The finding of the zero order solution is based on the CR isotropy during propagation in the space, whereas the anisotropy is taken into account when finding the next amendments. To begin with, the method is applied to solve the problem of CR modulation where the diffusion coefficient  $\kappa_0$  and the solar wind speed  $u$  are constants with LIS spectrum. The solution obtained with two iterations was compared with an analytical solution and with numerical solutions. Finally, solutions that have only one iteration for two problems of CR modulation with  $u = \text{const}$  and the same form of LIS spectrum were obtained and tested against numerical solutions. For the first problem,  $\kappa$  is proportional to the momentum of the particle  $p$ , so it has the form  $\kappa = \kappa_0 \eta$  where  $\eta = \frac{p}{m_0 c}$ . For the second problem, the diffusion coefficient is given in the form  $\kappa = k_0 \beta \eta$  where  $\beta = \frac{v}{c}$  is the particle speed relative to the speed of light. There was a good matching of the obtained solutions with the numerical solutions as well as with the analytical solution for the problem where  $\kappa = \text{const}$ .

**Key words:** cosmic rays – analytic method – exact solution of TPE equation – heliosphere

## 1 INTRODUCTION

The classic form of the equation of transport for cosmic rays (TPE) in a spherically symmetric interplanetary region without taking into account particle drift and any local sources has the form (Parker 1965; Gleeson and Axford 1967; Dolginov and Toptygin 1967, 1968; Jokipii and Parker 1970):

$$\frac{1}{r^2} \frac{\partial}{\partial r} \left( r^2 \kappa \frac{\partial f}{\partial r} \right) - u \frac{\partial f}{\partial r} + \frac{1}{3r^2} \frac{\partial}{\partial r} (r^2 u) \frac{\partial f}{\partial \ln p} = \frac{\partial f}{\partial t}, \quad (1)$$

where  $f(\mathbf{r}, p, t)$  is the omni-directional distribution function,  $\mathbf{r}$  is the radial distance from the Sun,  $p$  is the modulus of the momentum of the particle,  $t$  is time,  $u$  is the radial solar-wind

speed,  $\kappa(r, p, t)$  is the effective radial diffusion coefficient, i.e. it is  $\kappa_{rr}$ , which is the one from the nine elements of the diffusion tensor  $\mathbf{K}$ .

The omni-directional distribution function,  $f(\mathbf{r}, p, t)$  relates to the full CR distribution function,  $F(\mathbf{r}, \mathbf{p}, t)$  as

$$f(\mathbf{r}, p, t) = \frac{1}{4\pi} \int F(\mathbf{r}, \mathbf{p}, t) d\Omega \quad (2)$$

On the other hand, if particles are scattered by random inhomogeneities so that the angular distribution of the directions of the particles becomes isotropic, then it is possible to apply the diffusion approximation (Morse and Feshbach 1953) i.e. to use the moments of  $F(\mathbf{r}, \mathbf{p}, t)$ :

$$N(\mathbf{r}, p, t) = \int F(\mathbf{r}, \mathbf{p}, t) d\Omega \quad (3)$$

\* E-mail: kolesnyk@mao.kiev.ua

$$\mathbf{J}(\mathbf{r}, p, t) = \int F(\mathbf{r}, \mathbf{p}, t) \mathbf{v} d\Omega, \quad (4)$$

where  $N(\mathbf{r}, p, t)$  is the phase density of the particles and  $\mathbf{J}(\mathbf{r}, p, t)$  is the vector of the particle flux in space. The integration in (2), (3) and (4) is over the solid angle element  $d\Omega$  in momentum space. Thus taking into account (2) and (3) the TPE may be rewritten, as in Dolginov and Toptygin (1967, 1968), in a form involving  $N(\mathbf{r}, p, t)$ . Note that in the form was obtained by Dolginov and Toptygin (1967, 1968) from the kinetic Boltzman equation in which the regular as well as the random component of the interplanetary magnetic fields were taken into account. The in the such form can be represented as a continuity equation that describes the propagation of particles for a spherically symmetric event in phase space (Dorman et al. 1978; Gleeson and Webb 1978):

$$\nabla_r j_r + \nabla_p j_p = -\frac{\partial N(r, p, t)}{\partial t} \quad (5)$$

where  $\nabla_r = \frac{1}{r^2} \frac{\partial}{\partial r} r^2$  is the radial component of the divergence operator, and  $\nabla_p = \frac{1}{p^2} \frac{\partial}{\partial p} p^2$  is the component of the divergence operator in momentum space. The value

$$j_r = -\kappa(r, p, t) \frac{\partial N(r, p, t)}{\partial r} - \frac{up}{3} \frac{\partial N(r, p, t)}{\partial p} \quad (6)$$

is the CR flux in space, and

$$j_p = \frac{up}{3} \frac{\partial N(r, p, t)}{\partial r} \quad (7)$$

is the CR flux in momentum space. For stationary case, equation (5) describes CR propagation that is reduced to CR advection by the solar wind (SW). Particles with different energies are transferred with different rates that is described by term  $-\frac{up}{3} \frac{\partial N(r, p, t)}{\partial p}$  and on the other hand, CR penetrate diffusively into the SW with the rate  $\kappa(r, p, t) \frac{\partial N(r, p, t)}{\partial r}$ . This is accompanied by change in the particle energy which is determined by the balance between the oncoming and following encounters of particles with the moving irregularities of the interplanetary magnetic field ( $\frac{up}{3} \frac{\partial N(r, p, t)}{\partial r}$ ).

The possibility to obtain the exact analytical solutions (1) for various forms of  $\kappa$  and  $u$  (not including when (1) is greatly simplified for  $u \propto \frac{1}{r^2}$ ) has always attracted the attention of researchers. In this way, significant results were obtained, but only for steady-state case with  $u = \text{const}$  and involuntary forms of  $\kappa$ , i.e. form of  $\kappa$  which does not depend simultaneously on  $r$ ,  $p$  or  $R$  (the particle rigidity) and  $\beta$ , where  $\beta = \frac{v}{c}$  is the particle speed relative to the speed of light. In particular, analytic solutions have been derived by Dolginov and Toptygin (1967, 1968) for  $\kappa = \text{const}$  (see Appendix A, equation (A11)), by Fisk and Axford (1969) for  $\kappa = k_0 T^\alpha r^b$  ( $b > 1$ ,  $T$  is particle kinetic energy), by Webb and Gleeson (1977) for  $\kappa_0(p)r^b$  (via Green's Theorem and Green's function) and by Shakhov and Kolesnik

(2008) for  $\kappa_0 r^b$  (via Mellin transform). Attempts to obtain the exact analytical solution (1) for arbitrary forms of  $\kappa$  and  $u$  and especially for unsteady cases encounter into serious mathematical difficulties. Therefore, the development of the approximate analytical methods but with acceptable accuracy for the solving steady-state as well as time-dependent problems is an urgent problem. Furthermore, often is necessary to have the qualitative characteristics of the processes and the ability to freely operate by the variables in analytical formulas. This is a big advantage compared to the numerical calculations which, moreover, are almost always time-consuming.

## 2 ABOUT THE METHOD

In the present article we continue the development of an analytically iterative method for solving problems of CR modulation. The method was initially proposed by Shakhov and Kolesnyk (2006, 2009). The point of the method is as follows. Let us represent the particle density as the sum

$$N = N_0(r, p, t) + N_1(r, p, t) + N_2(r, p, t) + \dots \quad (8)$$

where  $N_0(r, p, t)$  is the zero order solution and  $N_{1,2,3,\dots}(r, p, t)$  are amendments to the zero solution. To obtain the zero order solution, we assume that the anisotropy of the CR during propagation in space is small, and that there is no radial CR flux at any point of space. This is the Force-Field approximation, which was initially introduced by Gleeson and Axford (1968) and furthered in (Gleeson and Urch 1973), which presented a new development for its solutions. At the boundary of the CR modulation ( $r_0$ ), for example at the heliosphere boundary, the zero order solution must satisfy a boundary condition involving its spectrum, for example be equal to some LIS spectrum. So, to find of the zero order solution, the following conditions must be satisfied:

$$\begin{cases} j_{r,0}(r, p, t) = 0, \\ N_0(r_0, p, t) = LIS. \end{cases} \quad (9)$$

The amendments to the zero order solution can be obtained from (5) by the following recurrence relation:

$$\nabla_r j_{r,i+1} + \nabla_p j_{p,i} = -\frac{\partial N_i(r, p, t)}{\partial t} \quad (10)$$

where  $i$  is an iteration index, which changes from the zero to infinity.

Taking into account (6) and (7) the last relation can be written in the following form:

$$\frac{1}{r^2} \frac{\partial}{\partial r} r^2 \left[ -\kappa \frac{\partial N_{i+1}}{\partial r} - \frac{up}{3} \frac{\partial N_{i+1}}{\partial p} \right] + \frac{1}{p^2} \frac{\partial}{\partial p} p^2 \left[ \frac{up}{3} \frac{\partial N_i}{\partial r} \right] = -\frac{\partial N_i}{\partial t} \quad (11)$$

Here, in order to obtain  $N_{i+1}$ , we will be guided by the fact that any radial CR flux (such as from the zero solution and

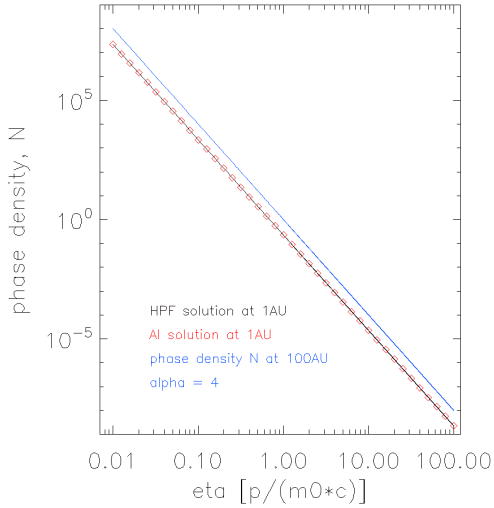


**Figure 1.** The comparison of the AI and HPF solutions at 1AU for the constant diffusion coefficient  $\kappa = 5.10^{18} m^2 s^{-1}$  and  $\alpha = 4$  (for more details see text)

also from the amendments) in the centre of the heliosphere (near the Sun) must be absent, i.e.  $j_{r,i}(0, p, t) = 0$ . This follows from the spherical symmetry of the problem. It should be noted that the amendments of the fluxes will be small but not equal to zero. This means that as more amendments are obtained, more of the CR anisotropy in the space will be taken into account. And the last condition is for finding  $N_{i+1}$ . As a common solution is presented in the form (8) and the zero solution  $N_0$  satisfies the boundary condition at  $r_0$ , this means that all amendments  $N_{i+1}$  at  $r_0$  must be equal to zero.

To sum up the above, for the finding of the amendments necessary to fulfil such conditions,

$$\begin{cases} j_{r,i+1}(0, p, t) = 0, \\ N_{i+1}(r_0, p, t) = 0. \end{cases} \quad (12)$$

Thus, in the first step, using (6) and (9) we may obtain the zero solution ( $N_0(r, p, t)$ ). Then, inserting it into (11) and applying (12), we obtain the first amendment ( $N_1(r, p, t)$ ). For obtaining the next amendment, it is necessary to put  $N_1(r, p, t)$  into (11) and again to apply (12), and so on. A common solution, as mentioned above, will be expressed in the form (8).

In the next chapters of this article we test the analytically iterative method (AI hereafter) for a constant diffusion coefficient and two shapes of non-constant diffusion coefficient.

We used the stochastic integration B-p method and the Crank-Nicolson method (CN hereafter) to verify the solutions obtained by AI. B-p is a stochastic integration method to solve the TPE backward in time. To find stochastic solutions of the Fokker-Planck equation (FPE), Itos lemma was used to rewrite the TPE into set of stochastic differential equations. This method historically is treated as a forward in time method of solution. The backward in time solution

was introduced by [Kota \(1977\)](#) and was given a detailed description in, for example by [Zhang \(1999\)](#). We apply the 1D backward stochastic integration method that is used, for example, by [Yamada et al. \(1998\)](#). A comparison of the backward and forward methods with a systematic error estimation for realistic LIS was published in ([Bobik et al. 2016](#)), where the B-p method is described in a detailed way.

CN is a numerical unconditionally stable finite difference method to solve FPEs ([Diaz 1958](#)). The method was proposed by [Fisk \(1971\)](#) to solve TPEs, and then used by many other authors. Here, the CN method is applied in the form in ([Batalha 2012](#)).

To compare the analytically iterative method, we use two completely independent numerical methods, to avoid any numerical artefacts or errors in the verification of the method.

### 3 A CONSTANT DIFFUSION COEFFICIENT

To verify the AI approach we start with the simpler case where the diffusion coefficient  $\kappa$  is constant. Obtaining a solution by AI method for  $\kappa = \text{const}$  and a LIS at the heliosphere boundary that has the form  $Cp^{-\alpha}$  is presented in Appendix A. A comparison with an analytical solution (see Equation(A11) in Appendix A) that is based on the confluent hypergeometric functions (HPF method hereafter) is available for this case, which therefore allows us to very accurately estimate the precision of the AI method. If not mentioned otherwise, all results published in this article were evaluated for protons in a spherically symmetric heliosphere with radius 100AU, where the SW has a speed of 400 km s<sup>-1</sup>.

In Figure 1, the phase density function  $N$  at 1AU is shown for  $\kappa = 5.10^{18} m^2 s^{-1}$  as are the slopes of the initial spectrum at the heliosphere boundary  $\alpha = 4$  evaluated by AI (red diamonds) and by HPF (black line), together with  $N$  at the modulation boundary (blue line). Both solutions are very similar at 1AU. The difference between them is on the order of 0.01 percent at all energies from  $\eta = 0.01$  ( $\eta = \frac{p}{m_0 c}$ , a proton with kinetic energy 47 keV) to  $\eta = 100$  (a proton with kinetic energy 92.89 GeV). As can be seen from Figure 1, the modulation is relatively the same for all energies because the diffusion coefficient does not depend on the energy. More precisely, by the modulation we mean the ratio between the phase density inside the heliosphere (here at 1AU) that normalised to the phase density for the same momentum at the modulation boundary (at 100AU). From Figure 1, we can see that difference between the solution that was obtained by AI and that obtained by HPF solution at the selected  $r$  does not depend on the energy.

We present in Figure 2 a comparison of the phase density spatial distribution across the heliosphere for selected energies, as evaluated by the AI, HPF, and CN methods. Presented are the ratios of the phase density functions evaluated for  $\kappa = 5.10^{18} m^2 s^{-1}$  and the slopes of the initial spectra at the heliosphere boundary  $\alpha = 3$  (in the left figure panel) and  $\alpha = 4$  (in the right figure panel). As for the case of constant  $\kappa$ , the ratio of AI/HPF does not depend on the energy (as can be seen from the AI solution and the exact solution(A11)), thus the ratios as functions of the radius for  $\eta = 1$  (388 MeV) and  $\eta = 10$  (8.49GeV) are very similar.

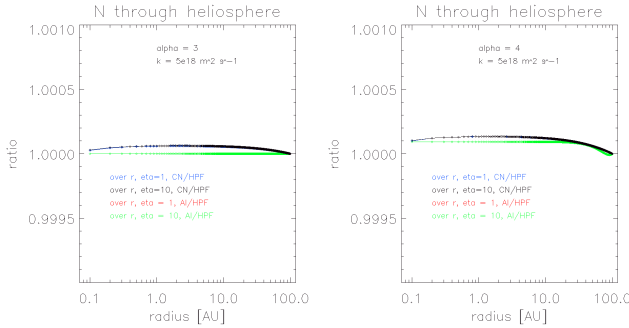


**Figure 2.** The comparison of the ratios of the AI, HPF and CN solutions as functions of the radius for the case of constant diffusion coefficient  $\kappa = 5.10^{18} \text{ m}^2 \text{ s}^{-1}$  and  $\alpha = 3$  (left panel) and  $\alpha = 4$  (right panel) (for more details see text)

Therefore the green line in the Figure 2 representing the ratio for  $\eta = 10$  hides the red line of the  $\eta = 1$  solution in both figure panels.

For the special case when  $\alpha = 3$  with the mentioned value of  $\kappa$ , the AI solution is very precise, with a difference between the AI and HPF solutions at a level of  $10^{-6}$  percent. This is due to the fact that for this case, the first amendment  $N_1$  and the second amendment  $N_2$  (as well as all higher amendments that will be found) are equal to zero (see Appendix A). As a result result, a common solution via AI is described by  $N_0$  alone (Equation(A3) in Appendix A) and is  $N_0 = C\eta^{-3} \exp[x - x_0]$ . Moreover, HPF describes Equation (A12) (see Appendix A) for this case. Therefore, HPF and AI yield identical solutions for  $\alpha = 3$ . The range for numerical error during the evaluation of the solutions is then very small. In Figure 2 we also show the ratios of the phase density functions evaluated by CN and HPF. CN in both cases attains a precision of 0.01 percent (precision as the difference from the analytic HPF solution). You can see that the AI solution for  $\alpha = 4$  is more precise than the CN solution. We evaluated the solutions for the same set of parameters also by the stochastic B-p method. The results from the B-p method confirmed the presented AI and HPF methods.

The precision of the AI solution depends on  $\kappa$  and slightly less on  $\alpha$ . In Figure 3, we present the dependence of the ratio between the AI and HPF solutions on  $\kappa$  at different distances  $r$ . For  $\alpha = 2$  and  $\alpha = 4$  the AI solutions are precise, on the order of 0.1 percents precision level, for diffusion coefficients  $\kappa$  greater than  $2.10^{18} \text{ m}^2 \text{ s}^{-1}$ . As could be expected, for  $\alpha = 3$  we see very high precision at every position inside the heliosphere for  $\kappa > 3.10^{17} \text{ m}^2 \text{ s}^{-1}$ . For  $\kappa = 2.10^{18} \text{ m}^2 \text{ s}^{-1}$  we evaluated the ratio of the AI and HPF solutions in dependence on  $\alpha$ . The results are presented in Figure 4. The precision decreases as  $\alpha$  becomes more different from 3 and with decreasing  $r$ .

It should be noted that the precision of the AI solution may be improved by finding more amendments (as mentioned in the description of the method) and by increasing the order of the summations in the evaluation of the amendments. This is true in the presented case for the first and the second amendments. The latter is understandable, due to the fact that we have applied a Taylor series expansion

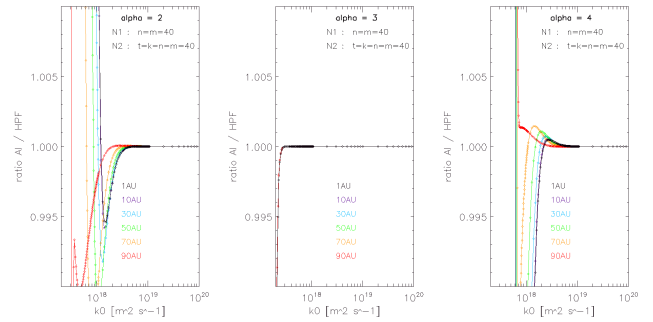


**Figure 3.** The comparison of the ratios of the AI and HPF solutions as functions of the value of a constant diffusion coefficient for  $\alpha = 2$  (left panel),  $\alpha = 3$  (middle panel) and  $\alpha = 4$  (right panel) (for more details see the text)

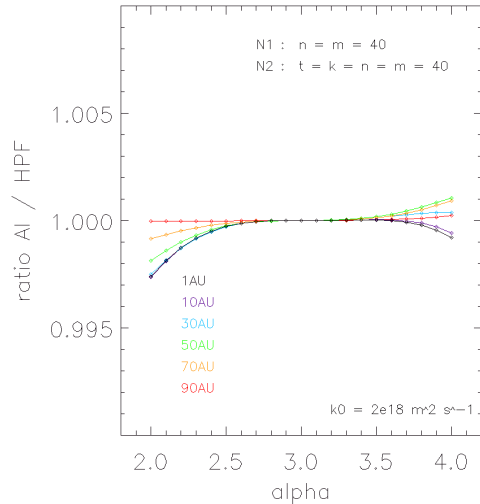


**Figure 4.** The comparison of the ratio of the AI and HPF solutions as functions of the initial spectrum slope  $\alpha$  for a constant  $\kappa$  (for more details see text)

for the exponential to obtain these amendments. But this has a limit due to limitations of the data types of computing languages. In particular, if a higher value of  $\frac{ur}{\kappa}$  is used, then the number of terms in the sums in  $N_1$  and  $N_2$  must be increased in order to attain acceptable accuracy. As a result, this situation significantly increases the time for the evaluation of the amendments.

## 4 NON-CONSTANT DIFFUSION COEFFICIENT

### 4.1 Solution for $\kappa = k_0\eta$

The solution for the case of a non-constant diffusion coefficient with shape  $\kappa = k_0\eta$  was derived in Appendix B on the basis of the AI method. Here it should be noted that although  $N_1$  (see equation (B9)) is expressed through integrals

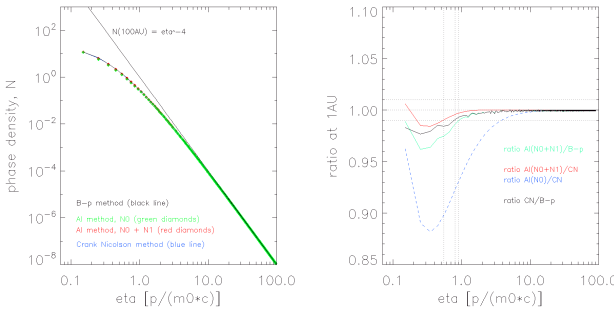


**Figure 5.** The comparisons of the AI, B-p and the CN solutions at 1AU for  $k_0 = 5 \cdot 10^{18} \text{ m}^2 \text{s}^{-1}$ ,  $\alpha = 4.0$  and  $\kappa = k_0 \eta$  (for more details see text)

but to construct the corresponding curve is sufficient to use one of the mathematical packages such as Maple, Mathematica, MATLAB etc. In this case result will be faster than the numerical calculation of such a problem. And at the same for numerical calculations (for CN as well as the B-p stochastic method) of the problem should use or apply the program code to obtain the required points. And after by means of their, we can build the appropriate curve.

An analytical solution for this shape of the diffusion coefficient and power law unmodulated spectrum is not available. In particular it should be noted that for similar problem where for  $\kappa = k_0 p^\alpha$  was obtained by Cowsik and Lee (1977) an analytical solution only for the constant solar wind speed and for a specific form of LIS spectrum but not for arbitrary form. Herewith, the form of LIS spectrum that was examined is not a power law kind.

We compared the AI solutions, i.e.  $N_0$  and  $N_0 + N_1$ , with the solutions provided by CN and the B-p stochastic method. By using two independent numerical methods (B-p and CN) we want to ensure the validity of the comparison with the AI method.

In Figure 5 the comparison of the solutions for energies starting from  $\eta = 0.15$  (T=11 MeV) at 1AU for  $\alpha = 4.0$  and  $k_0 = 5 \cdot 10^{18} \text{ m}^2 \text{s}^{-1}$  is presented. The zero order solution  $N_0$  is indicated in the figure by  $AI(N_0)$  and the sum of the zero order solution and the first amendment  $N_0 + N_1$  is indicated by  $AI(N_0 + N_1)$ . Over a wide range of energies, all four solutions, i.e.  $N_0$ ,  $N_0 + N_1$ , CN, and B-p in Figure 5 are similar. As can be seen from the right panel of Figure 5, comparisons of the AI solution with that of the CN method, and of the AI solution with that B-p, show that the difference is less than 1 percent for energies higher than 324 MeV ( $\eta > 0.9$ ). The CN and AI solutions are more similar than the AI and B-p solutions. The ratio  $AI/CN$  remains within the one percent difference range for energies higher than 133 MeV ( $\eta > 0.55$ ). The CN solution and the B-p solution differ by less than 1 percent over a wide range of energies: from 263 MeV ( $\eta = 0.8$ ) to higher energies.

To look more closely at the precision of the AI solution, we compare the solutions provided by the AI and CN methods at 1AU for a range of values of the diffusion coefficient and for the selected slopes of the power law unmodulated spectrum at 100AU. In Figure 6 the ratios between the AI and CN solutions at 1AU for different  $\kappa_0$  and  $\alpha = 3.0, 4.0$  and

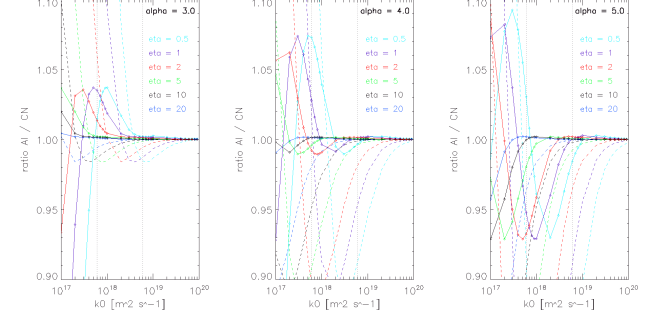


**Figure 6.** The comparison of AI and CN solutions ratio for different diffusion coefficients  $k_0$  and  $\alpha = 3$  (left panel),  $\alpha = 4$  (middle panel) and  $\alpha = 5$  (right panel) at 1AU for  $\eta = 0.5, 1, 2, 5, 10, 20$ . Dotted lines represents ratio of  $AI(N_0)/CN$  solutions, solid lines represents  $AI(N_0 + N_1)/CN$ . AI and CN for  $\kappa = k_0 \eta$  (for more details see text)

5.0 and selected energies are shown. The dotted lines represent the ratio of the solutions  $AI(N_0)/CN$ , the solid lines represent the ratio  $AI(N_0 + N_1)/CN$ . Here,  $AI(N_0)$  is the zero order solution and  $AI(N_0 + N_1)$  is the sum of the zero order solution and the first amendment. The ratios become closer to unity with increasing values of  $\kappa_0$ . We can see from the figure that when  $k_0$  is larger than  $2 \cdot 10^{17} \text{ m}^2 \text{s}^{-1}$ , then all  $AI(N_0 + N_1)$  differ from the CN solutions by less than 1 percent for energies over  $\eta = 20$  (17.85GeV) and in the range of  $\alpha$  tested. Also, for  $k_0$  larger than  $2 \cdot 10^{18} \text{ m}^2 \text{s}^{-1}$ , all AI solutions differ from CN solutions by less than 1 percent for energies over  $\eta = 2$  (1.16GeV).

## 4.2 Solution for $\kappa = k_0 \beta \eta$

The solution for a non-constant diffusion coefficient with shape  $\kappa = k_0 \beta \eta$  and for power law unmodulated spectrum is derived in Appendix C. The comparison of the AI solutions with the solutions that were obtained by the CN and B-p methods for energies starting from  $\eta = 0.1$  (T=5 MeV) at 1AU for  $k_0 = 5 \cdot 10^{18} \text{ m}^2 \text{s}^{-1}$  and  $\alpha = 4.0$  is presented in Figure 7.

The ratios of the AI solution to CN and B-p solutions for the zero order solution  $N_0$  (indicated by  $AI(N_0)$ ) and for the common solution that consist of the zero solution and the first amendment  $N_0 + N_1$  (indicated by  $AI(N_0 + N_1)$ ) are shown in the figure's right panel.

From inspection of the figure, we can see that the common AI solution differs by less than one percent from the CN solution for energies bigger than 79 MeV ( $\eta > 0.42$ ). The B-p solution stays within the one percent difference region from energies 349 MeV ( $\eta > 0.94$ ), but for smaller energies it oscillates around the two percent difference region.

The precision of the AI solution for different values of  $k_0$  for  $\kappa = k_0 \beta \eta$  was similarly reviewed, as in the previous two diffusion cases. As one can see from Figure 8, the ratio  $AI/CN$  goes to unity with increasing values of the two factors, namely with  $k_0$  and the energy. But with increasing  $\alpha$ , the situation is slightly the opposite and ambiguous. For example, there is about a three percent difference between

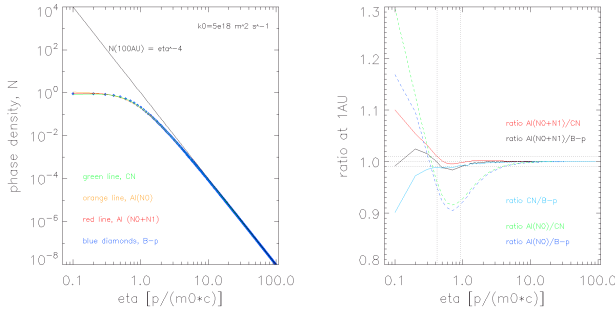


**Figure 7.** The comparison of the AI, B-p and CN solutions at 1AU for  $k_0 = 5 \cdot 10^{18} \text{ m}^2 \text{s}^{-1}$ ,  $\alpha = 4.0$  and  $\kappa = k_0 \beta \eta$  (for more details see text)

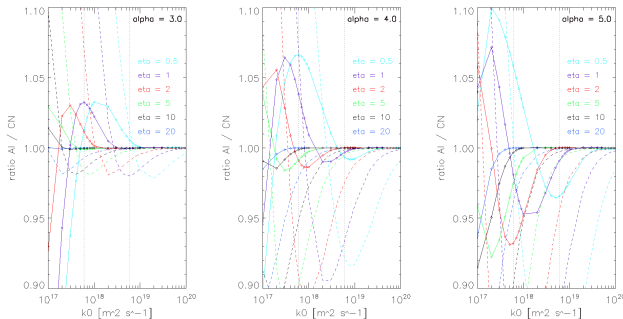


**Figure 8.** The comparison of the ratio of the AI and CN solutions for different diffusion coefficients  $k_0$  and  $\alpha = 3$  (left panel),  $\alpha = 4$  (middle panel) and  $\alpha = 5$  (right panel) at 1AU for  $\eta = 0.5, 1, 2, 5, 10, 20$ . Dashed lines represent the ratio  $AI(N_0)/CN$ , solid lines represent  $AI(N_0 + N_1)/CN$ . AI and CN for  $\kappa = k_0 \beta \eta$  (for more details see the text)

the AI and CN solutions when  $\alpha = 3$  for an energy of 111 MeV ( $\eta = 0.5$ ) and  $k_0 = 1 \cdot 10^{18} \text{ m}^2 \text{s}^{-1}$ , and the difference is already about 5.5% when  $\alpha = 4$  for the same energy and  $k_0$ . But when  $\alpha = 5$ , then the difference again becomes 3% for the same parameters. The situation is similar for the other energies.

For example, when the energy is 1.16 GeV ( $\eta = 2$ ) and  $k_0 = 4 \cdot 10^{17} \text{ m}^2 \text{s}^{-1}$ , the differences are 2% for  $\alpha = 3$ , 1% for  $\alpha = 4$ , and 6.5% for  $\alpha = 5$ . Here it should be noted that if the modulation parameter  $x_0$  ( $x_0 = \frac{u r_0}{k_0}$ ) is less than 10, i.e. when  $k_0 > 6 \cdot 10^{17} \text{ m}^2 \text{s}^{-1}$ , then the deviation of the AI solution from the CN solution reaches no more than 6% for any checked  $\alpha$  and energy. We think this is a good result taking into account that numerical methods also have accuracy limits, as can be seen from the ratio CN/B-p (Figure 7).

Finally, the dependence of the precision of the solution on  $\alpha$  at 1AU for two selected  $k_0$  is presented in Figure 9. The values used for  $k_0$  were chosen as the border values of the modulation range, between a very strong maximum and a weak minimum of the solar cycle.  $k_0$  was evaluated from the modulation strength  $\phi$  (Usoskin et al. 2005, 2010). The weakest modulation during the 22 and 23 solar cycle occurred in February 1987 (22 solar cycle) with  $\phi = 311 \text{ MV}$ . From the average SW speed in February 1987,  $u = 5.08 \cdot 10^5$

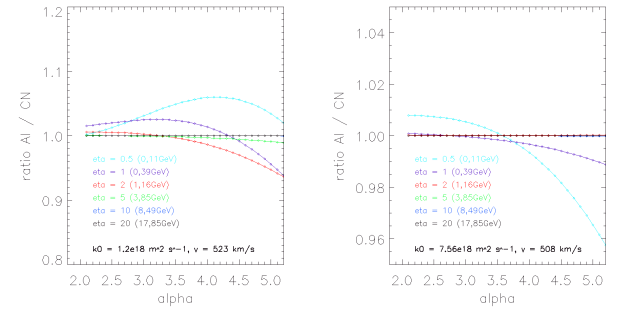


**Figure 9.** The comparison of the ratio of the AI and CN solutions as functions of the initial spectrum slope  $\alpha$  at 1AU for two selected values of  $k_0$ . Solutions for  $\kappa = k_0 \beta \eta$  (for more details see the text)

$\text{ms}^{-1}$  (OMNIweb) we found that  $k_0 = 7.56 \cdot 10^{18} \text{ m}^2 \text{s}^{-1}$ . The strongest modulation during solar cycles 22 and 23 occurred in June 1991 with  $\phi = 2016 \text{ MV}$ ,  $u = 5.23 \cdot 10^5 \text{ ms}^{-1}$ , which leads to  $k_0 = 1.2 \cdot 10^{18} \text{ m}^2 \text{s}^{-1}$ . Using these two values of  $k_0$  we can show the precision of the evaluated methods for a range of values appearing in the last solar cycles. During very strong modulations in solar maxima, when  $k_0$  reaches the smallest values, the AI/CN ratios stay within the one percent difference range for energies over 3.85 GeV ( $\eta > 5$ ) for all tested values of  $\alpha$  (see left panel in Figure 9). The precision is one order of magnitude better during solar minima, when  $k_0$  reaches its highest values. As we can see in the right panel of Figure 9, the precision is better than 0.1 percent for energies higher than 1.16 GeV ( $\eta > 2$ ) for all tested  $\alpha$ . It should be noted that the difference is less than the six percent between AI and CN for the solar minima period as well as for the solar maxima period for all tested energies and  $\alpha$ .

Let us note, that we published codes of models used in this article on the web page [www.CRmodels.org](http://www.CRmodels.org).

## 5 DISCUSSION AND CONCLUSIONS

In this paper we have obtained solutions for three steady-state problems of CR modulation by means of an analytically iterative method. By summing all three cases, we can reach the following conclusion. The accuracy of these solutions at a given point  $r$  is more dependent on a value of the modulation parameter  $x_0$  ( $x_0 = \frac{u r_0}{\kappa}$  for the problem where  $\kappa = \text{const}$  and  $x_0 = \frac{u r_0}{k_0}$  for problems where  $\kappa = k_0 \eta$  or  $\kappa = k_0 \beta \eta$ ) than on the choice of the slope of the initial spectrum  $\alpha$ .

Thus, for  $x_0 < 10$ , the obtained solutions have minimal differences in accuracy in comparison with numerical solutions and exact solution for the problem when  $\kappa = \text{const}$ . In particular, for the problem where the diffusion coefficient is a constant, so that  $x_0 = 1.2$  (i.e. when  $k_0 = 5 \cdot 10^{18} \text{ m}^2 \text{s}^{-1}$ ,  $u = 4 \cdot 10^5 \text{ m}^2 \text{s}^{-1}$  and  $r_0 = 100 \text{ AU}$ ) the obtained AI solution is even closer to the exact solution than its numerical solution. For a task where the diffusion coefficient is proportional to the momentum and for the same value of  $x_0$ , we have shown that the AI solution deviates from the numerical solution CN

**Table 1.** The estimates of the errors (in %) of the Force-Field solutions and AI solutions in comparison with HPF and with the numerical solutions at 1AU for  $u = 4 \cdot 10^5 \text{ m}^2\text{s}^{-1}$ ,  $\alpha = 4$  and for various  $x_0$  (for more details see the the text).

	$\kappa = \text{const}$				$\kappa = k_0\eta$				$\kappa = k_0\beta\eta$			
	$\frac{N_0}{\text{HPF}}$	$\frac{N_0+N_1}{\text{HPF}}$	$\frac{N_0+N_1+N_2}{\text{HPF}}$	$\frac{\text{HPF}}{\text{CN}}$	$\frac{N_0}{\text{CN}}$	$\frac{N_0+N_1}{\text{CN}}$	$\frac{N_0}{B-p}$	$\frac{N_0+N_1}{B-p}$	$\frac{N_0}{\text{CN}}$	$\frac{N_0+N_1}{\text{CN}}$	$\frac{N_0}{B-p}$	$\frac{N_0+N_1}{B-p}$
$x_0 = 1.2$	7.7	-0.001	-0.009	-0.17	10.7	1.13	12.16	2.66	6.58	-0.1	7.77	1.17
$x_0 = 3$	31	3.9	0.08	-0.04	9.25	0.52	6.54	-1.55	-2.71	-2.77	0.31	0.26
$x_0 = 5$	55.3	17.1	2.9	0.71	-2.78	-3.03	3.24	3.24	-12.1	-5	-8.05	-1.13
$x_0 = 6.5$	69	30.6	8.8	0.96	-8.77	-4.63	-7.36	-0.74	-18.2	-5.92	-21.12	-8.47
$x_0 = 9$	83.9	53.6	26.1	1.94	-21.8	-6.82	-15.01	2.21	-26.7	-6.57	-43.38	-20.51

by not more than 1.55% over the entire considered range of energies and the deviation is less than 1% starting from energies of  $T = 133 \text{ MeV}$  ( $\eta = 0.55$ ). For the problem where  $\kappa = k_0\beta\eta$ , the deviation of the AI solution from the numerical solution CN is less than 1% beginning already at an energy of  $T = 79 \text{ MeV}$  ( $\eta = 0.42$ ), which is better than for the previous problem. It should be noted that although the comparison of the AI solution with the numerical solution B-p is more advantageous for this case (the B-p solution has a deviation of not more than 2.5% over all of the investigated range of energies) and less profitable for  $\kappa = k_0\eta$ , here we have provided only one of them because the difference between the two numerical methods can reach 10%, as seen from Figure 7. It should also be noted that the situation with the obtained AI solutions at smaller values of  $x_0$ , i.e.  $x_0 < 1$ , is even better than the above examined case.

In this paper we evaluated the possible  $x_0$  values during real physical conditions, as an example, we have chosen different cycles of solar activity. The maximum  $x_0$  value that we have found available during maximum solar activity does not exceed  $x_0 = 6.5$  (i.e. when  $k_0 = 1.2 \cdot 10^{18} \text{ m}^2\text{s}^{-1}$ ,  $u = 5.23 \cdot 10^5 \text{ m}^2\text{s}^{-1}$  and  $r_0 = 100\text{AU}$ ). In very rare situations, when there is a very fast SW and a low value of  $k_0$ , then  $x_0$  may reach a value over 10.

In this case, the difference between the AI and numerical solutions becomes larger but at the same time gives us much better accuracy than the Force-Field solutions ( $N_0$ ). This result is shown in Table 1 and Table 2, estimates of the errors (in %) of  $N_0$  and AI solutions in comparison with HPF (only for the problem where  $\kappa = \text{const}$  there is an exact solution) and numerical solutions at 1AU for  $u = 4 \cdot 10^5 \text{ m}^2\text{s}^{-1}$  and  $\alpha = 4$  for various cases. In this table the case  $\kappa = \text{const}$  corresponds to the exact HPF solution only. Therefore Table 1 demonstrates estimates for all three problems mentioned above. The parameters were chosen as follows:  $x_0 = 1.2, 3, 5, 6.5, 9$ ; energy  $\eta = 0.5$  ( $\kappa = k_0\eta$  and  $\kappa = k_0\beta\eta$ ). Table 2 displays estimates for the cases when  $\kappa$  is not constant (for  $x_0 = 1.2$ ) and for various energies that are higher than  $\eta = 0.2$ . These tables show the importance of inclusion the one amendment  $N_1$  in comparison with the Force-Field solution for the selected  $x_0$  (Table 1) and for the selected  $\eta$  (Table 2). The result is even better when the second amendment is also taken into account (for the problem with  $\kappa = \text{const}$ ). We can see that accuracy deteriorates with the increasing  $x_0$  (for all the three problems) and with the decreasing  $\eta$  (for the problems where  $\kappa$  is not constant).

Therefore we think that using more amendments in this method would produce more accurate solutions for those

rare occasions of  $x_0$ , when it is necessary. To show it and also that the common iterative solution (8) converges with the exact solution was examined a problem in Appendix E where LIS has the time dependence. For this purpose was taken into account a term  $\frac{\partial N_i}{\partial t}$  in (11). In addition it has been shown that the exact solution of the considered problem is unknown because of the difficulty to carry out the inverse Laplace transform for (E2), therefore the AI method in this situation as and for another problems has big advantage.

So we believe that the obtained solutions for the considered problems by means of proposed method can be regarded as analytical solutions of such problems with some remarks. The method can be widely applied for solving the various steady-states and non-stationary problems of CR modulation with almost arbitrary dependences of the SW speed, forms of LIS spectrum and the diffusion coefficient ( $\kappa$ ) which is simultaneously dependent on  $p$  (or  $R$ ),  $\beta$  and  $r$ . Depending on  $u$  and/or  $\kappa$  the proposed method may have some restrictions. This is why we have used above the word "almost". To find at least the zero order solution of (6) we should solve the transcendental equation which at the same time depends on  $u$ ,  $\kappa$ . Usually it is difficult to solve analytically or even not possible. For example, if  $u = \text{const}$  and we choose a form  $k$  such as  $\kappa = k_0(1 + \eta + \eta^2)$ , when we insert them into (6) we will obtain an equation which may be solved only by a numerical way. Here it should be noted that "1" in the form  $\kappa$  "prevents" to solve this example analytically. We guess other the restrictions on the use of the method do not exist.

We think that by means of proposed approach is possible to theoretically examine a stationary model of the spherically symmetric heliosphere to describe the physical processes during CRs propagation therein (Kolesnik and Shakhov 2012; Kota and Jokipii 2014; Fedorov 2015). The model includes an environment that consist of two adjacent to each other spherically symmetric (relative to the Sun) regions. Internal part of the heliosphere is limited by a termination shock (TS) which placed at  $r_0$  from the Sun, the radial SW speed is constant and supersonic,  $V_{in}$  but  $\kappa$  has a form:  $\kappa = k_1\beta\eta\frac{r}{r_0}$ . Beyond TS, the SW speed jumps to a value  $V_{in}/3$  (Richardson and Burlaga 2013) and spreads with deceleration in the outer part of the heliosphere (the heliosheath) that is limited by the heliopause (HP). Such deceleration can be presented in the form of a power law depending on the heliocentric distance with index 'n', i.e.:  $V_{ihs} = \frac{V_{in}}{3} \cdot \left(\frac{r}{r_0}\right)^{-n}$ , here  $\kappa$  has the form which was considered in this article:  $\kappa = k_2\beta\eta$ , where  $k_1$  and  $k_2$  may be determined from data received by the Voyager 1. Due to the absence of the SW speed inside the interstellar medium

**Table 2.** The estimates of the errors (in %) of the Force-Field solutions and AI solutions in comparison with the numerical solutions for problems where  $\kappa = k_0\eta$  and  $\kappa = k_0\beta\eta$  with  $x_0 = 1.2$  ( $r = 1\text{AU}$ ,  $u = 4 \cdot 10^5 \text{ m}^2\text{s}^{-1}$ ,  $k_0 = 5 \cdot 10^{18} \text{ m}^2\text{s}^{-1}$ ),  $\alpha = 4$  and for energies higher than  $\eta = 0.2$  ( $T = 19 \text{ MeV}$ ) (for more details see the the text).

	$\kappa = k_0\eta$				$\kappa = k_0\beta\eta$			
	$\frac{N_0}{CN}$	$\frac{N_0+N_1}{CN}$	$\frac{N_0}{B-p}$	$\frac{N_0+N_1}{B-p}$	$\frac{N_0}{CN}$	$\frac{N_0+N_1}{CN}$	$\frac{N_0}{B-p}$	$\frac{N_0+N_1}{B-p}$
$\eta = 0.2$ ( $T = 19 \text{ MeV}$ )	7.36	0.45	8.14	2.08	-12.73	-5.38	-9.6	-2.45
$\eta = 0.3$ ( $T = 41 \text{ MeV}$ )	11.4	1.55	13.23	3.7	-2.98	-3.13	-1.39	-1.54
$\eta = 0.4$ ( $T = 72 \text{ MeV}$ )	11.53	1.44	13.18	3.23	3.22	-1.23	4.27	-0.12
$\eta = 0.5$ ( $T = 111 \text{ MeV}$ )	10.7	1.13	12.16	2.66	6.58	-0.1	7.77	1.17
$\eta = 0.6$ ( $T = 156 \text{ MeV}$ )	9.67	0.84	11.15	2.37	8.06	0.37	9.01	1.39
$\eta = 0.7$ ( $T = 207 \text{ MeV}$ )	8.67	0.61	9.92	1.89	8.45	0.47	9.53	1.65
$\eta = 0.8$ ( $T = 263 \text{ MeV}$ )	7.76	0.44	8.69	1.38	8.25	0.41	9.13	1.37
$\eta = 0.9$ ( $T = 324 \text{ MeV}$ )	6.97	0.32	7.73	1.07	7.77	0.29	8.51	1.09
$\eta = 1$ ( $T = 389 \text{ MeV}$ )	6.28	0.23	6.89	0.84	7.18	0.17	7.82	0.86
$\eta = 2$ ( $T = 1.16 \text{ GeV}$ )	2.68	-0.0008	2.9	0.22	2.94	-0.18	3.31	0.21
$\eta = 5$ ( $T = 3.85 \text{ GeV}$ )	0.64	0.003	0.63	-0.005	0.59	-0.08	0.71	0.04
$\eta = 10$ ( $T = 8.49 \text{ GeV}$ )	0.19	0.006	0.22	0.04	0.15	-0.04	0.18	-0.01
$\eta = 20$ ( $T = 17.85 \text{ GeV}$ )	0.05	0.005	0.08	0.03	0.03	-0.02	0.06	0.01

(beyond HP), the phase density of the particles will be determined by only the diffusion process under the constant diffusion coefficient. Note, that [Kota and Jokipii \(2014\)](#) and [Fedorov \(2015\)](#) considered the easier mathematical problem, when  $n = 2$  ( $\nabla \cdot \mathbf{V} = 0$ , i.e. beyond the TS, no adiabatic energy changes occur for CRs). It should be noted here that, although  $\nabla \cdot \mathbf{V}$  for large  $n$  in the heliosheath is very small quantity, it is not equal to zero. In this case the third term in (1) will be proportional to  $\nabla \cdot \mathbf{V} \cdot \eta \frac{\partial N}{\partial \eta}$ . This means that neglecting the whole term is not correct, as its contribution may be significant for a range of low energy particles ( $\eta < 1$ ). In a numerical way, this effect was shown by [Langner et al. \(2006\)](#) where the symmetrical two-dimensional model for different scenarios  $V_{ihs}$  in the heliosheath was studied. In particular, it was shown there that changing the profiles for  $V_{ihs}$  has a noteworthy effect on barrier modulation at low energies and that the barrier at such energies in the heliosheath is wider and deeper for the  $V_{ihs} \propto \frac{1}{r^8}$  scenario than for  $V_{ihs} \propto \frac{1}{r^2}$ . In this way, by the method, we think there is possible to derive a solution of the problem for given above the diffusion coefficients as well as with the arbitrary  $n$  to look at possible effects with the theoretical side.

The method may be applied for the theoretically description of time-dependent CR modulation too, i.e. at long-term time on which we can observe solar cycle related changes in cosmic ray intensities due to changes in the modulation environment ([Manuel et al. 2011](#)). For this purpose need be taken into account a time-dependent term in (11) and changes in the modulation environment will be described by the diffusion coefficient that varies with time.

We also think that the proposed method may be the significant step to create analytical approach to solve two-dimensional (2D) (dependence from the radial distance and a polar angle) with taking into account particle drift.

## ACKNOWLEDGEMENTS

We are grateful to the referee for his/her constructive comments.

This work was supported in part by the National Scholarship Programme of the Slovak Republic for the Support of the Mobility of Students, PhD Students, University Teachers, Researchers and Artists (Yu.L.K.).

This work was partially supported by the Slovak Academy of Sciences, grant MVTS JEM-EUSO.

## REFERENCES

Batalha L., 2012, Solar Modulation effects on Cosmic Rays  
 Bateman H., and Erdelyi A., 1953, Higher Transcendental Functions. Vol. 1.  
 Cowsik R., and M.A. Lee, 1977, ApJ, 216:635-645  
 Diaz, J. B., 1958, John Wiley, New York, pp. 14-64  
 Bobik P., et al., 2016, J. Geophys. Res., V. 121, Issue 5, pp. 3920-3930  
 Dolginov, A.Z., and I.N. Toptygin, 1967, Geomagnetizm i Aeronomiya 7, 967  
 Dolginov, A.Z., and I. N. Toptygin, 1968, Icarus, 8, 54  
 Dorman, L. I., M. E. Kats, Yu.I. Fedorov, and B.A. Shakhov, 1978, Pis'ma Zh. Ehksp. Teor. Fiz., vol. 27, pp. 374-378  
 Fisk, L. A., and W.I. Axford, 1969, J. Geophys. Res., 74, 4973.  
 Fisk, L. A., 1971, J. Geophys. Res., 76 (1), 221-226, doi:10.1029/JA076i001p00221.  
 Fedorov, Yu.I., 2015, Kinematics and Physics of Celestial Bodies, V. 31, Issue 3, pp 105-118, doi: 10.3103/S0884591315030034.  
 Gleeson, L.J., and W.I. Axford, 1967, ApJ, 149, L115-L118  
 Gleeson, L.J., and W.I. Axford, 1968, ApJ, 154, 1011  
 Gleeson, L.J., and I.A. Urch, 1973, Ap&SS, 25, 387  
 Gleeson, L.J., G.M. Webb, 1978, Ap&SS, 58, 21  
 Jokipii, J.R., and E.N. Parker, 1970, ApJ, 160, 735-744  
 Kolesnik, Yu.L., and B.A. Shakhov, 2012, Kinematics and Physics of Celestial Bodies, V.28, issue 6, P.261-269, doi:10.3103/S0884591312060049  
 Kota, J., 1977, ICRC, 15th, Plovdiv, Bulgaria, August 13-26, 1977

Kota, J. and J.R. Jokipii, 2014, Are cosmic rays modulated beyond the heliopause, *ApJ*, 782, doi:10.1088/0004-637X/782/1/24

Langner, U. W., M.S. Potgieter, H. Fichtner and T. Borrmann, 2006, *ApJ*, 640: 1119-1134

Manuel R., S.E.S. Ferreira, M.S. Potgieter, R.D. Strauss, N.E. Engelbrecht, 2011, *Advances in Space Research*, 47, 1529-1537

Morse, P. M., Feshbach, H. (1953). *Methods of Theoretical Physics. International Series in Pure and Applied Physics*, New York: McGraw-Hill

Parker, E.N., 1965, *Planet. Space Sci.*, 13, 9-49

Richardson, J.D. and L.F. Burlaga, 2013, *Space Sci. Rev.*, 176:217-235, doi: 10.1007/s11214-011-9825-5

Shakhov, B.A., and Yu.L. Kolesnyk, 2006, *Kinematika i Fizika Nebesnykh Tel*, vol. 22, no. 2, pp. 101-108

Shakhov, B.A., and Yu.L. Kolesnik, 2008, *Kinematics and Physics of Celestial Bodies*, V. 24, issue 6, P.280-292, doi:10.3103/S0884591308060032

Shakhov, B.A., and Yu.L. Kolesnyk, 2009, *Proceedings of 21st European Cosmic Ray Symposium*, pp.245-247

Usoskin, I.G., K. Alanko-Huotari, G. A. Kovaltsov, and K. Mursula, 2005, *J. Geophys. Res.*, vol. 110, A12108, doi:10.1029/2005JA011250

Usoskin, I.G. G.A. Bazilevskaya, and G. A. Kovaltsov, 2010, *J. Geophys. Res.*, vol. 116, A02104, doi:10.1029/2010JA016105

Webb, G.M. and L.J. Gleeson, 1977, *Ap&SS*, 50, 205W

Yamada, Y., S. Yanagita, and T. Yoshida, 1998, *Geophys. Res. Lett.*, 25, 2353-2356, doi:10.1029/98GL51869.

Zhang, M., 1999, *ApJ*, 513, 409-420, doi:10.1086/306857.

OMNIweb, <http://omniweb.gsfc.nasa.gov/form/dx1.html>

## APPENDIX A: $\kappa = \text{const}$

To obtain a solution of the problem, we introduce the following dimensionless variables:  $x = \frac{ur}{\kappa}$ ,  $x_0 = \frac{ur_0}{\kappa}$  and  $\eta = \frac{p}{m_0 c}$ . Then taking into account (6) and (9), we obtain a system of equations for finding the zero order solution:

$$\begin{cases} \frac{\partial N_0(x, \eta)}{\partial x} + \frac{\eta}{3} \frac{\partial N_0(x, \eta)}{\partial \eta} = 0, \\ N_0(x_0, \eta) = C\eta^{-\alpha}. \end{cases} \quad (\text{A1})$$

The last system of equations can be rewritten in the following form

$$\begin{cases} N_0(x, \eta) = f(\eta \exp(-\frac{x}{3})), \\ N_0(x_0, \eta) = C\eta^{-\alpha}. \end{cases} \quad (\text{A2})$$

Then the solution of the last system has the form

$$N_0 = C\eta^{-\alpha} \exp\left[\frac{\alpha}{3}(x - x_0)\right] \quad (\text{A3})$$

To obtain the first and next amendments, we use a form such as  $N_i = C\eta^{-\alpha}\Phi_i(x)$ , and when we insert  $N_0$  into (11) we will obtain an equation for  $N_1$ :

$$\frac{1}{x^2} \frac{d}{dx} x^2 \left[ -\frac{d\Phi_1}{dx} + \frac{\alpha}{3} \Phi_1 \right] + \frac{\alpha(3 - \alpha)}{9} \exp\left[\frac{\alpha}{3}(x - x_0)\right] = 0 \quad (\text{A4})$$

If we expand the exponent in the last equation in a Taylor

series, we obtain

$$\frac{d\Phi_1}{dx} - \frac{\alpha}{3} \Phi_1 = \frac{\alpha(3 - \alpha)}{9} \exp\left(-\frac{\alpha}{3}x_0\right) \sum_{n=0}^{\infty} \frac{(\frac{\alpha}{3})x^{n+1}}{n!(n+3)} \quad (\text{A5})$$

Here, there was applied the first condition (12), i.e. the integration was carried out from 0 to  $x$ . We will seek a solution of the last equation in the following form:

$$\Phi_1 = B \exp\left(\frac{\alpha x}{3}\right) + \exp\left(\frac{\alpha x}{3}\right) \int_0^x \exp\left(-\frac{\alpha x}{3}\right) \frac{\alpha(3 - \alpha)}{9} \cdot \exp\left(-\frac{\alpha}{3}x_0\right) \sum_{n=0}^{\infty} \frac{(\frac{\alpha}{3})x^{n+1}}{n!(n+3)} dx \quad (\text{A6})$$

After expansion of the exponent in a series and an integration, we get

$$\Phi_1 = B \exp\left(\frac{\alpha x}{3}\right) + \frac{\alpha(3 - \alpha)}{9} \exp\left(\frac{\alpha}{3}(x - x_0)\right) \cdot \sum_{n=0}^{\infty} \sum_{m=0}^{\infty} \frac{(-1)^m (\frac{\alpha}{3})^{n+m} x^{n+m+2}}{n!m!(n+3)(n+m+2)} \quad (\text{A7})$$

The last condition (12) for finding  $B$  was used, i.e.  $\Phi_1(x_0) = 0$  and then  $B$  has following form:

$$B = -\frac{\alpha(3 - \alpha)}{9} \exp\left(-\frac{\alpha}{3}x_0\right) \sum_{n=0}^{\infty} \sum_{m=0}^{\infty} \frac{(-1)^m (\frac{\alpha}{3})^{n+m} x_0^{n+m+2}}{n!m!(n+3)(n+m+2)} \quad (\text{A8})$$

And as a result, the first amendment is

$$N_1 = C\eta^{-\alpha} \exp\left[\frac{\alpha}{3}(x - x_0)\right] \frac{\alpha(3 - \alpha)}{9} \cdot \sum_{n=0}^{\infty} \sum_{m=0}^{\infty} \frac{(-1)^m (\frac{\alpha}{3})^{n+m} (x^{n+m+2} - x_0^{n+m+2})}{n!m!(n+m+2)(n+3)} \quad (\text{A9})$$

When we perform similar actions in order to find the second amendment, we will get

$$\begin{aligned} N_2 &= C\eta^{-\alpha} \exp\left[\frac{\alpha}{3}(x - x_0)\right] \frac{\alpha(3 - \alpha)^2}{27} \cdot \sum_{t=0}^{\infty} \sum_{k=0}^{\infty} \sum_{n=0}^{\infty} \sum_{m=0}^{\infty} \frac{(-1)^{m+t} (\frac{\alpha}{3})^{n+m+k+2}}{t!k!n!m!(n+m+2)(n+3)} \cdot \\ &\cdot \left[ \frac{n+m+k+2}{(n+m+k+4)(n+m+k+t+3)} (x^{n+m+k+t+3} - x_0^{n+m+k+t+3}) - \frac{k \cdot x_0^{n+m+2}}{(k+2)(k+t+1)} (x^{k+t+1} - x_0^{k+t+1}) \right] \end{aligned} \quad (\text{A10})$$

An exact solution for this problem was initially obtained by Dolginov and Toptygin (1967). In our notation, it has the following form:

$$N_{e.s.} = C\eta^{-\alpha} \frac{F(\frac{2\alpha}{3}, 2; x)}{F(\frac{2\alpha}{3}, 2; x_0)} \quad (\text{A11})$$

where  $F(a, b; x)$  is the confluent hypergeometrical function (Bateman and Erdelyi 1953). In particular, from the property of the confluent hypergeometrical function, it follows that for the simpler case when  $\alpha = 3$  the exact solution (A11) has the form:

$$N_{e.s., \alpha=3} = C\eta^{-3} \exp[x - x_0] \quad (\text{A12})$$

## APPENDIX B: $\kappa = k_0\eta$

To obtain a solution for the problem, we introduce the following dimensionless variables:  $x = \frac{ur}{k_0}$ ,  $x_0 = \frac{u r_0}{k_0}$  and  $\eta = \frac{p}{m_0 c}$ . Then taking into account (6) and (9), we obtain a system of equations for finding the zero order solution:

$$\begin{cases} \frac{\partial N_0(x, \eta)}{\partial x} + \frac{1}{3} \frac{\partial N_0(x, \eta)}{\partial \eta} = 0, \\ N_0(x_0, \eta) = A\eta^{-\alpha}. \end{cases} \quad (\text{B1})$$

The last system can be rewritten in the following form:

$$\begin{cases} N_0(x, \eta) = f(\eta - \frac{x}{3}), \\ N_0(x_0, \eta) = A\eta^{-\alpha}. \end{cases} \quad (\text{B2})$$

Then the solution of the last system has the form:

$$N_0 = A \left[ \eta - \frac{x - x_0}{3} \right]^{-\alpha} \quad (\text{B3})$$

After inserting  $N_0$  into (11), we will obtain an equation for  $N_1$ :

$$\frac{1}{x^2} \frac{\partial}{\partial x} x^2 \left[ -\eta \frac{\partial N_1}{\partial x} - \frac{\eta}{3} \frac{\partial N_1}{\partial \eta} \right] = -\frac{\alpha A}{9\eta^2} \frac{\partial}{\partial \eta} \left[ \eta^3 \left( \eta - \frac{x - x_0}{3} \right)^{-\alpha-1} \right] \quad (\text{B4})$$

After differentiating the left hand side of the last equation, we get

$$-\frac{\partial N_1}{\partial x} - \frac{1}{3} \frac{\partial N_1}{\partial \eta} = I \quad (\text{B5})$$

where

$$\begin{aligned} I = & -\frac{\alpha A}{9\eta x^2} \int_0^x \left( \eta - \frac{\xi - x_0}{3} \right)^{-\alpha-1} \cdot \\ & \cdot \left[ 3 - \eta(\alpha + 1) \cdot \left( \eta - \frac{\xi - x_0}{3} \right)^{-1} \right] \xi^2 d\xi \end{aligned} \quad (\text{B6})$$

Here, the limits of integration were selected as being from 0 to  $x$  in consequence of the applying of the first condition (12). Now, we consider the integral  $I$  separately. If we define  $y = \eta - \frac{\xi - x_0}{3}$  and then the expression for  $I$  can be

rewritten in the following form:

$$\begin{aligned} I = & -\frac{\alpha A}{3\eta x^2} \int_{\eta - \frac{x - x_0}{3}}^{\eta + \frac{x_0}{3}} y^{-\alpha-1} \left[ 3 - \eta(\alpha + 1)y^{-1} \right] \cdot \\ & \cdot [3\eta - 3y + x_0]^2 dy = \\ = & -\frac{\alpha A}{3\eta x^2} \left( \frac{27}{-\alpha + 2} \left[ \left( \eta + \frac{x_0}{3} \right)^{-\alpha+2} - \left( \eta - \frac{x - x_0}{3} \right)^{-\alpha+2} \right] + \right. \\ & + \frac{9[\eta(7 + \alpha) + 2x_0]}{\alpha - 1} \left[ \left( \eta + \frac{x_0}{3} \right)^{-\alpha+1} - \left( \eta - \frac{x - x_0}{3} \right)^{-\alpha+1} \right] - \\ & - \frac{3[3\eta + x_0] \cdot [\eta(5 + 2\alpha) + x_0]}{\alpha} \cdot \\ & \cdot \left[ \left( \eta + \frac{x_0}{3} \right)^{-\alpha} - \left( \eta - \frac{x - x_0}{3} \right)^{-\alpha} \right] + \\ & \left. + \eta(3\eta + x_0)^2 \left[ \left( \eta + \frac{x_0}{3} \right)^{-\alpha-1} - \left( \eta - \frac{x - x_0}{3} \right)^{-\alpha-1} \right] \right) \end{aligned} \quad (\text{B7})$$

Whereas  $N_0$  has the form (B3), then, by with taking into account the second condition (12), it is necessary to search for a  $N_1$  of the following form:

$$N_1 = \int_x^{x_0} f(x \rightarrow \xi, \eta \rightarrow \eta - \frac{x - \xi}{3}) d\xi \quad (\text{B8})$$

And as the result the first amendment takes the following form:

$$\begin{aligned} N_1 = & -\frac{\alpha A}{3} \cdot \int_x^{x_0} \left( \frac{27}{-\alpha + 2} \frac{\left[ \eta - \frac{x - \xi - x_0}{3} \right]^{-\alpha+2} - \left[ \eta - \frac{x - x_0}{3} \right]^{-\alpha+2}}{\xi^2(\eta - \frac{x - \xi}{3})} \right. \\ & + \frac{9}{\alpha - 1} \frac{\left[ \eta - \frac{x - \xi - x_0}{3} \right]^{-\alpha+1} - \left[ \eta - \frac{x - x_0}{3} \right]^{-\alpha+1}}{\xi^2(\eta - \frac{x - \xi}{3})} \cdot \\ & \cdot \left[ (\eta - \frac{x - \xi}{3})(7 + \alpha) + 2x_0 \right] - \frac{3}{\alpha} \frac{\left[ \eta - \frac{x - \xi - x_0}{3} \right]^{-\alpha} - \left[ \eta - \frac{x - x_0}{3} \right]^{-\alpha}}{\xi^2(\eta - \frac{x - \xi}{3})} \cdot \\ & \cdot \left[ 3(\eta - \frac{x - \xi}{3}) + x_0 \right] \left[ (\eta - \frac{x - \xi}{3})(5 + 2\alpha) + x_0 \right] + \\ & \left. + \frac{\left[ \eta - \frac{x - \xi - x_0}{3} \right]^{-\alpha-1} - \left[ \eta - \frac{x - x_0}{3} \right]^{-\alpha-1}}{\xi^2} \left[ 3(\eta - \frac{x - \xi}{3}) + x_0 \right]^2 \right) d\xi \end{aligned} \quad (\text{B9})$$

It should be noted that  $N_1$  is not defined for  $\alpha = 0, 1, 2$ .

## APPENDIX C: $\kappa = k_0\beta\eta$

To obtain a solution for the problem, we introduce the following dimensionless variables:  $x = \frac{ur}{k_0}$ ,  $x_0 = \frac{u r_0}{k_0}$  and  $\eta = \frac{p}{m_0 c}$ . Note that for such a problem, the diffusion coefficient  $\kappa$  can be rewritten in the following form:  $\kappa = k_0 \frac{\eta^2}{\sqrt{\eta^2 + 1}}$ . This follows from the fact that  $p = \frac{V E}{c^2}$  and  $E = \sqrt{p^2 c^2 + m_0^2 c^4}$ . Taking into account (6) and (9), we obtain a system of equations for finding the zero order solution:

$$\begin{cases} \frac{\eta}{\sqrt{\eta^2+1}} \frac{\partial N_0(x, \eta)}{\partial x} + \frac{1}{3} \frac{\partial N_0(x, \eta)}{\partial \eta} = 0, \\ N_0(x_0, \eta) = A\eta^{-\alpha}. \end{cases} \quad (\text{C1})$$

The last system can be rewritten in the form

$$\begin{cases} N_0(x, \eta) = f(\sqrt{\eta^2+1} - \frac{x}{3}), \\ N_0(x_0, \eta) = A\eta^{-\alpha}. \end{cases} \quad (\text{C2})$$

Then the solution of the last system has the form

$$N_0 = A \left( \sqrt{\left[ \sqrt{\eta^2+1} - \frac{x-x_0}{3} \right]^2 - 1} \right)^{-\alpha} \quad (\text{C3})$$

After inserting  $N_0$  into (11), we will obtain an equation for  $N_1$ :

$$\begin{aligned} \frac{1}{x^2} \frac{\partial}{\partial x} x^2 \left[ \frac{\eta^2}{\sqrt{\eta^2+1}} \frac{\partial N_1}{\partial x} + \frac{\eta}{3} \frac{\partial N_1}{\partial \eta} \right] = -\frac{\alpha A}{3}. \\ \left( \left[ \sqrt{\eta^2+1} - \frac{x-x_0}{3} \right]^2 - 1 \right)^{-\frac{\alpha}{2}-1} \cdot \left[ \sqrt{\eta^2+1} - \frac{x-x_0}{3} + \right. \\ \left. + \frac{\eta^2}{3\sqrt{\eta^2+1}} \cdot \frac{(\alpha+1)(\sqrt{\eta^2+1} - \frac{x-x_0}{3})^2 + 1}{1 - (\sqrt{\eta^2+1} - \frac{x-x_0}{3})^2} \right] \end{aligned} \quad (\text{C4})$$

After introducing the variable:  $\theta = \sqrt{\eta^2+1}$  and simplifying the last equation, we get:

$$\begin{aligned} -\frac{\partial N_1}{\partial x} - \frac{1}{3} \frac{\partial N_1}{\partial \theta} = -\frac{\alpha A}{3x^2(\theta^2-1)} \left[ \left( \frac{4\theta^2-1}{3} + \frac{x_0\theta}{3} \right) \cdot K - \frac{\theta}{3} \cdot L - \right. \\ \left. - \frac{(\alpha+2)(\theta^2-1)}{3} \cdot M \right] \end{aligned} \quad (\text{C5})$$

where

$$\begin{aligned} K &= \int_0^x \left( \left[ \theta - \frac{x-x_0}{3} \right]^2 - 1 \right)^{-\frac{\alpha}{2}-1} \cdot x^2 dx; \\ L &= \int_0^x \left( \left[ \theta - \frac{x-x_0}{3} \right]^2 - 1 \right)^{-\frac{\alpha}{2}-1} \cdot x^3 dx; \\ M &= \int_0^x \left( \left[ \theta - \frac{x-x_0}{3} \right]^2 - 1 \right)^{-\frac{\alpha}{2}-2} \cdot \left[ \theta - \frac{x-x_0}{3} \right]^2 \cdot x^2 dx. \end{aligned}$$

Note that the limits of integration in  $K$ ,  $L$ ,  $M$  were selected as being from 0 to  $x$  in consequence of applying of the first condition (12). The detailed calculation of the integrals was shown in Appendix D.

Due to the fact that the solution of the homogeneous equation (C5) has the form  $f(\theta - \frac{x}{3})$ , and taking into account the second condition (12), it is necessary to search for a  $N_1$  in the following form:

$$N_1 = \int_x^{x_0} f \left( x \rightarrow \xi, \theta \rightarrow \theta - \frac{x-\xi}{3} \right) d\xi \quad (\text{C6})$$

By taking into account the form for  $N_1$  (C6) and also

using (C5), we obtain

$$\begin{aligned} N_1 = -\frac{\alpha A}{9} \int_x^{x_0} \frac{d\xi}{\xi^2 \cdot ((\theta - \frac{x-\xi}{3})^2 - 1)} \left[ \left( 4(\theta - \frac{x-\xi}{3})^2 + \right. \right. \\ \left. \left. + x_0(\theta - \frac{x-\xi}{3}) - 1 \right) K(x \rightarrow \xi, \theta \rightarrow \theta - \frac{x-\xi}{3}) - (\theta - \frac{x-\xi}{3}) \cdot \right. \\ \left. \cdot L(x \rightarrow \xi, \theta \rightarrow \theta - \frac{x-\xi}{3}) - (\alpha+2)((\theta - \frac{x-\xi}{3})^2 - 1) \cdot \right. \\ \left. \cdot M(x \rightarrow \xi, \theta \rightarrow \theta - \frac{x-\xi}{3}) \right] \end{aligned} \quad (\text{C7})$$

## APPENDIX D: CALCULATION OF THE INTEGRALS $K$ , $L$ , $M$

For the calculation of the integrals  $K$ ,  $L$ ,  $M$  from Appendix C, let us first consider the integral  $I$  that has the following form:

$$I = \int z^k (z^2 - 1)^\beta dz \quad (\text{D1})$$

if we represent  $(z^2 - 1)^\beta$  as a sum, i.e.  $(z^2 - 1)^\beta = \sum_{n=0}^{\infty} (-1)^n \cdot C_\beta^n \cdot (z^2)^{\beta-n}$  where  $C_\beta^n$  is the binomial coefficient (which can be represented through the Gamma function  $\Gamma$  as  $C_\beta^n = \frac{\Gamma(\beta+1)}{\Gamma(\beta-n+1) \cdot n!}$ ), we can apply here properties of  $\Gamma$  such as  $\frac{\Gamma(\beta+1)}{\Gamma(\beta-n+1)} = \frac{\Gamma(n-\beta)}{\Gamma(-\beta)} (-1)^n$  and see that  $I$  assumes the following form:

$$I = -\frac{z^{k+2\beta+1}}{2} \cdot \sum_{n=0}^{\infty} \frac{\Gamma(n-\beta)}{\Gamma(-\beta) \cdot n! (n-\beta - \frac{k}{2} - \frac{1}{2})} z^{-2n} \quad (\text{D2})$$

If we now use the fact that  $\Gamma(z) = z \cdot \Gamma(z+1)$  and multiply (D2) by  $\frac{\Gamma(-\frac{k}{2} + \frac{1}{2} - \beta)}{\Gamma(-\frac{k}{2} - \frac{1}{2} - \beta)}$ , then we get

$$\begin{aligned} I &= -\frac{z^{k+2\beta+1}}{2} \cdot \frac{\Gamma(-\frac{k}{2} - \frac{1}{2} - \beta)}{\Gamma(-\frac{k}{2} + \frac{1}{2} - \beta)} \cdot \\ &\cdot \sum_{n=0}^{\infty} \frac{\Gamma(-\beta+n) \cdot \Gamma(n - \frac{k}{2} - \frac{1}{2} - \beta) \cdot \Gamma(-\frac{k}{2} + \frac{1}{2} - \beta)}{\Gamma(-\beta) \cdot n! \cdot \Gamma(n - \frac{k}{2} + \frac{1}{2} - \beta) \cdot \Gamma(-\frac{k}{2} - \frac{1}{2} - \beta)} z^{-2n} \end{aligned} \quad (\text{D3})$$

For the last expression, we can apply the definition of hypergeometrical function  $F(a, b; c; z)$  (Bateman and Erdelyi 1953):  $F(a, b; c; z) = \sum_{n=0}^{\infty} \frac{\Gamma(a+n)}{\Gamma(a)} \cdot \frac{\Gamma(b+n)}{\Gamma(b)} \cdot \frac{\Gamma(c)}{\Gamma(c+n)} \cdot \frac{z^n}{n!}$ . Finally, we obtain

$$\int z^k (z^2 - 1)^\beta dz = \frac{z^{k+1+2\beta}}{k+1+2\beta} \cdot F(-\beta, -\frac{k}{2} - \frac{1}{2} - \beta; -\frac{k}{2} + \frac{1}{2} - \beta; z^{-2}) \quad (\text{D4})$$

And now, to use (D4) to find the integrals  $K$ ,  $L$ ,  $M$ , we introduce the substitution in these integrals:  $\theta - \frac{x-x_0}{3} = z$ . As a result, these integrals take the following form:

$$K = 27 \cdot \int_{\theta - \frac{x-x_0}{3}}^{\theta + \frac{x_0}{3}} (z^2 - 1)^{-\frac{\alpha}{2}-1} \cdot (z^2 - 2\omega z + \omega^2) dz;$$

$$L = -81 \cdot \int_{\theta - \frac{x-x_0}{3}}^{\theta + \frac{x_0}{3}} (z^2 - 1)^{-\frac{\alpha}{2} - 1} \cdot (z^3 - 3\omega z^2 + 3\omega^2 z - \omega^3) dz;$$

$$M = 27 \cdot \int_{\theta - \frac{x-x_0}{3}}^{\theta + \frac{x_0}{3}} (z^2 - 1)^{-\frac{\alpha}{2} - 2} \cdot (z^4 - 2\omega z^3 + \omega^2 z^2) dz,$$

where  $\omega = \theta + \frac{x_0}{3}$ . Eventually, if we apply (D4) to each of these integrals, we obtain

$$K = \left[ \frac{27}{1-\alpha} z^{1-\alpha} F\left(\frac{\alpha}{2} + 1, \frac{\alpha}{2} - \frac{1}{2}; \frac{\alpha}{2} + \frac{1}{2}; \frac{1}{z^2}\right) + \frac{54}{\alpha} \omega z^{-\alpha} \cdot F\left(\frac{\alpha}{2} + 1, \frac{\alpha}{2}; \frac{\alpha}{2} + 1; \frac{1}{z^2}\right) - \frac{27}{\alpha + 1} \omega^2 z^{-\alpha - 1} \cdot F\left(\frac{\alpha}{2} + 1, \frac{\alpha}{2} + \frac{1}{2}; \frac{\alpha}{2} + \frac{3}{2}; \frac{1}{z^2}\right) \right]_{\theta - \frac{x - x_0}{3}}^{\theta + \frac{x_0}{3}} \quad (D5)$$

$$\begin{aligned}
L = & \left[ \frac{81}{\alpha-2} z^{2-\alpha} F\left(\frac{\alpha}{2}+1, \frac{\alpha}{2}-1; \frac{\alpha}{2}; \frac{1}{z^2}\right) + \frac{243}{1-\alpha} \omega z^{1-\alpha} \cdot \right. \\
& \cdot F\left(\frac{\alpha}{2}+1, \frac{\alpha}{2}-\frac{1}{2}; \frac{\alpha}{2}+\frac{1}{2}; \frac{1}{z^2}\right) + \frac{243}{\alpha} \omega^2 z^{-\alpha} \cdot \\
& \cdot F\left(\frac{\alpha}{2}+1, \frac{\alpha}{2}; \frac{\alpha}{2}+1; \frac{1}{z^2}\right) - \frac{81}{\alpha+1} \omega^3 z^{-\alpha-1} \cdot \\
& \left. \cdot F\left(\frac{\alpha}{2}+1, \frac{\alpha}{2}+\frac{1}{2}; \frac{\alpha}{2}+\frac{3}{2}; \frac{1}{z^2}\right) \right]_{\theta-\frac{x-x_0}{3}}^{\theta+\frac{x_0}{3}} \quad (D6)
\end{aligned}$$

$$M = \left[ \frac{27}{-\alpha + 1} z^{-\alpha+1} F\left(\frac{\alpha}{2} + 2, \frac{\alpha}{2} - \frac{1}{2}; \frac{\alpha}{2} + \frac{1}{2}; \frac{1}{z^2}\right) + \frac{54}{\alpha} \omega z^{-\alpha} F\left(\frac{\alpha}{2} + 2, \frac{\alpha}{2}; \frac{\alpha}{2} + 1; \frac{1}{z^2}\right) - \frac{27}{\alpha + 1} \omega^2 z^{-\alpha-1} F\left(\frac{\alpha}{2} + 2, \frac{\alpha}{2} + \frac{1}{2}; \frac{\alpha}{2} + \frac{3}{2}; \frac{1}{z^2}\right) \right]_{\theta - \frac{x-x_0}{3}}^{\theta + \frac{x_0}{3}} \quad (D7)$$

## APPENDIX E:

## $\kappa = \text{const}$ AND LIS HAS THE TIME DEPENDENCE

Let's consider a problem when the diffusion coefficient ( $\kappa$ ) is constant inside the heliosphere but LIS has a form:  $N_0(r_0, \eta, t) = f(t)\eta^{-\alpha}$ , i.e. LIS has dependency from time and the momentum of the particle on boundary of the heliosphere  $r_0$ . Like for example such dependence may be considered during a supernova explosion, when the density of the particles varies on border of the heliosphere with time. To obtain solutions, i.e. as an exact solution as well as by means of the method, we introduce the following dimensionless variables:  $x = \frac{ur}{\kappa}$ ,  $x_0 = \frac{ur_0}{\kappa}$ ,  $\eta = \frac{p}{m_0 c}$  and  $\tau = \frac{u^2 t}{\kappa}$ .

The exact solution of the problem may be obtained if to solve a system of equations:

$$\begin{cases} \frac{1}{x^2} \frac{\partial}{\partial x} x^2 \left[ -\frac{\partial N(x, \eta, \tau)}{\partial x} - \frac{\eta}{3} \frac{\partial N(x, \eta, \tau)}{\partial \eta} \right] + \\ + \frac{1}{3\eta^2} \frac{\partial}{\partial \eta} \left[ \eta^3 \frac{\partial N(x, \eta, \tau)}{\partial x} \right] = -\frac{\partial N(x, \eta, \tau)}{\partial \tau}, \\ N(x_0, \eta, \tau) = f(\tau) \eta^{-\alpha}. \end{cases}$$

Here, the first equation is TPE in a form (1) with taking into account the dimensionless variables and the second

equation is the boundary condition. If to apply the Laplace transform, i.e.  $N(x, \eta, s) = \int_0^\infty \exp(-s\tau)N(x, \eta, \tau)d\tau$  to the last system, we get

$$\begin{cases} \frac{\partial^2 N(x, \eta, s)}{\partial x^2} + \left(\frac{2}{x} - 1\right) \frac{\partial N(x, \eta, s)}{\partial x} + \frac{2\eta}{3x} \frac{\partial N(x, \eta, s)}{\partial \eta} = sN(x, \eta, s), \\ N(x_0, \eta, s) = F(s)\eta^{-\alpha}. \end{cases} \quad (E1)$$

Let us note that during integrating of the right hand side of the last system, we used the fact that there is no the phase density at the initial time, i.e.  $N(x, \eta, 0) = 0$ . The solution of the last system has the following form:

$$N(x, \eta, s) = F(s)\eta^{-\alpha} \cdot \exp\left[-\frac{1}{2}(x - x_0)(\sqrt{4s+1} - 1)\right] \cdot \frac{F(1 + \frac{2\alpha-3}{3\sqrt{4s+1}}, 2; \sqrt{4s+1}x)}{F(1 + \frac{2\alpha-3}{3\sqrt{4s+1}}, 2; \sqrt{4s+1}x_0)} \quad (E2)$$

If we expand the exponent and the confluent hypergeometrical function in the last equation in a Taylor series and restrict ourselves by the second order  $x$  and  $x_0$  in such expansion, we obtain

$$\begin{aligned}
& N(x, \eta, s) = F(s)\eta^{-\alpha} \cdot \\
& \cdot \frac{1 + (1 - \sqrt{4s + 1})\frac{x}{2} + (1 - \sqrt{4s + 1})^2\frac{x^2}{8} + \dots}{1 + (1 - \sqrt{4s + 1})\frac{x_0}{2} + (1 - \sqrt{4s + 1})^2\frac{x_0^2}{8} + \dots} \cdot \\
& \cdot \frac{1 + \frac{3\sqrt{4s+1}+2\alpha-3}{6}x + \frac{(3\sqrt{4s+1}+2\alpha-3)(6\sqrt{4s+1}+2\alpha-3)}{108}x^2 + \dots}{1 + \frac{3\sqrt{4s+1}+2\alpha-3}{6}x_0 + \frac{(3\sqrt{4s+1}+2\alpha-3)(6\sqrt{4s+1}+2\alpha-3)}{108}x_0^2 + \dots} = \\
& = F(s)\eta^{-\alpha} \cdot \frac{1 + \frac{\alpha}{3}x + (\frac{1}{6}s + \frac{1}{18}\alpha + \frac{1}{27}\alpha^2)x^2 + \dots}{1 + \frac{\alpha}{3}x_0 + (\frac{1}{6}s + \frac{1}{18}\alpha + \frac{1}{27}\alpha^2)x_0^2 + \dots} \quad (E3)
\end{aligned}$$

Now, divide the numerator of (E3)  $(1 + \frac{\alpha}{3}x + (\frac{1}{6}s + \frac{1}{18}\alpha + \frac{1}{27}\alpha^2)x^2 + \dots)$  on the denominator of (E3)  $(1 + \frac{\alpha}{3}x_0 + (\frac{1}{6}s + \frac{1}{18}\alpha + \frac{1}{27}\alpha^2)x_0^2 + \dots)$  in a column

$$\begin{aligned}
 & \frac{1 + \frac{\alpha}{3}x + (\frac{1}{6}s + \frac{1}{18}\alpha + \frac{1}{27}\alpha^2)x^2}{1 + \frac{\alpha}{3}x_0 + (\frac{1}{6}s + \frac{1}{18}\alpha + \frac{1}{27}\alpha^2)x_0^2} \Bigg|_{x=x_0} \\
 & \frac{- \frac{\alpha}{3}(x - x_0) + (\frac{1}{6}s + \frac{1}{18}\alpha + \frac{1}{27}\alpha^2)(x^2 - x_0^2)}{\frac{\alpha}{3}(x - x_0) + \frac{\alpha^2}{9}x_0(x - x_0) + \dots} \\
 & \frac{- (\frac{1}{6}s + \frac{1}{18}\alpha)(x^2 - x_0^2) - \frac{\alpha^2}{9}x_0x + \frac{\alpha^2}{27}(x^2 + 2x_0^2)}{(\frac{1}{6}s + \frac{1}{18}\alpha)(x^2 - x_0^2) - \frac{\alpha^2}{9}x_0x + \frac{\alpha^2}{27}(x^2 + 2x_0^2)} \\
 & \qquad \qquad \qquad 0 + \dots
 \end{aligned}$$

And as the result the analytical image of the problem with retaining till the second order of  $x$  and  $x_0$  has the following form:

$$N(x, \eta, s) = F(s)\eta^{-\alpha} \cdot \left[ 1 + \frac{\alpha}{3}(x - x_0) - \frac{\alpha^2}{9}x_0x + \left( \frac{1}{6}s + \frac{1}{18}\alpha(x^2 - x_0^2) + \frac{\alpha^2}{27}(x^2 + 2x_0^2) \right) \right] \quad (\text{E4})$$

To obtain the analytical solution for the problem, necessary to apply the inverse Laplace transform, i.e.  $f(\tau) = \frac{1}{2\pi i} \int_{\sigma_1-i\infty}^{\sigma_1+i\infty} \exp(s\tau)F(s)ds$ . Note that in contrast to (E2) this approach can be readily done for the last equation subject to the restriction that has been done above. As result, we obtain an analytic solution for the problem:

$$N(x, \eta, \tau) = \eta^{-\alpha} \left[ 1 + \frac{\alpha}{3}(x - x_0) - \frac{\alpha^2}{9}x_0x + \frac{1}{18}\alpha(x^2 - x_0^2) + \frac{\alpha^2}{27}(x^2 + 2x_0^2) \right] f(\tau) + \eta^{-\alpha} \left[ \frac{x^2 - x_0^2}{6} \right] \frac{\partial f(\tau)}{\partial \tau} \quad (\text{E5})$$

Now we try to find a solution the problem by the AI method. Then taking into account (6) and (9), we obtain a system of equations for finding the zero order solution:

$$\begin{cases} \frac{\partial N_0(x, \eta, \tau)}{\partial x} + \frac{\eta}{3} \frac{\partial N_0(x, \eta, \tau)}{\partial \eta} = 0, \\ N_0(x_0, \eta, \tau) = f(\tau)\eta^{-\alpha}. \end{cases} \quad (\text{E6})$$

The image of the zero order solution has a similar form as and (A3) for a problem that was detailed considered in Appendix A:

$$N_0(x, \eta, s) = F(s)\eta^{-\alpha} \exp\left[\frac{\alpha}{3}(x - x_0)\right] \quad (\text{E7})$$

To obtain the first amendment, we use a form such as a  $N_1 = \eta^{-\alpha}\Phi_1(x)$ , and when we insert  $N_0$  into (11) we obtain an equation for the image of  $N_1$ :

$$\begin{aligned} \frac{1}{x^2} \frac{d}{dx} x^2 \left[ -\frac{d\Phi_1}{dx} + \frac{\alpha}{3}\Phi_1 \right] + \frac{\alpha(3-\alpha)}{9} \exp\left[\frac{\alpha}{3}(x - x_0)\right] = \\ = -sF(s) \exp\left[\frac{\alpha}{3}(x - x_0)\right] \end{aligned} \quad (\text{E8})$$

When we fulfill the same actions that were done in Appendix A during the obtaining of  $N_1$ , we finally get:

$$\begin{aligned} N_1(x, \eta, s) = F(s)\eta^{-\alpha} \left[ \frac{\alpha(3-\alpha)}{9} + s \right] \exp\left[\frac{\alpha}{3}(x - x_0)\right] \cdot \\ \cdot \sum_{n=0}^{\infty} \sum_{m=0}^{\infty} \frac{(-1)^m \left(\frac{\alpha}{3}\right)^{n+m} (x^{n+m+2} - x_0^{n+m+2})}{n!m!(n+m+2)(n+3)} \end{aligned} \quad (\text{E9})$$

If to expand the exponents in a series with retaining till

the second order of  $x$  and  $x_0$  as it has been done in finding analytical solution, we get

$$\begin{aligned} N_0(x, \eta, s) + N_1(x, \eta, s) = F(s)\eta^{-\alpha} \cdot \\ \left[ 1 + \frac{\alpha}{3}(x - x_0) + \frac{\alpha^2}{18}(x^2 + x_0^2) - \frac{\alpha^2}{9}x_0x \right] + \\ + F(s)\eta^{-\alpha} \left[ \frac{\alpha}{18}(x^2 - x_0^2) - \frac{\alpha^2}{54}(x^2 - x_0^2) + \frac{s}{6}(x^2 - x_0^2) \right] = \\ = F(s)\eta^{-\alpha} \left[ 1 + \frac{\alpha}{3}(x - x_0) - \frac{\alpha^2}{9}x_0x + \right. \\ \left. + \left( \frac{s}{6} + \frac{\alpha}{18} \right)(x^2 - x_0^2) + \frac{\alpha^2}{27}(x^2 + 2x_0^2) \right] \end{aligned} \quad (\text{E10})$$

It should be noted that here we restricted ourselves to only the first amendment because of following amendments will contain  $x$  and  $x_0$  higher than the second order as it can be seen in Appendix A.

It can be seen that every term of the image of the AI solution (E10) coincides with the corresponding term of the analytical image (E4). Of course, their own solutions are identical to each other, i.e. are (E5). Furthermore, if to examine our problem till the first order  $x$  and  $x_0$ , so we see that the first three terms of the image (E10) (that included in the  $N_0$ ) coincide the first three terms of image (E4). This indicates that the common iterative solution (8) corresponds and converges with the exact solution. In other words using more amendments by means of the AI method would bring closer to the exact solution of the considered problem.

This paper has been typeset from a  $\text{TeX}/\text{L}\text{A}\text{T}\text{E}\text{X}$  file prepared by the author.